Tarım Makinaları Bilimi Dergisi (Journal of Agricultural Machinery Science)
2011, 7 (2), 165-169

An Images Analysis Technique for Recognition of Brown Leaf Spot Disease in Cassava

Wanrat ABDULLAKASIM[1], Kittipong POWBUNTHORN[1], Jintana UNARTNGAM[2], Tomohiro TAKIGAWA[3]
[1]Department of Agricultural Engineering, Faculty of Engineering at Kamphaengsaen, Kasetsart University, Nakhon Pathom 73140 THAILAND
[2]Department of Plant Pathology, Faculty of Agriculture at Kamphaengsaen, Kasetsart University, Nakhon Pathom 73140 THAILAND
[3]Graduate School of Life and Environmental Sciences, University of Tsukuba, Ibaraki 305-8572 JAPAN
Tel.: +66–34–351–896; E-mail: fengwra@ku.ac.th

Received (Geliş Tarihi): 08.05.2011 Accepted (Kabul Tarihi): 10.07.2011

Abstract: An automated computer vision system to monitor epidemic development of plant pathogens is important in site-specific crop protection. The objective of this study was to develop an image analysis technique for the detection of brown leaf spot (BLS) disease caused by *Cercosporidium henningsii* Allesch in cassava (*Manihot esculenta* Crantz). Color images of healthy and diseased cassava leaves were captured in fields with a resolution of 640×480 pixels and further cropped into blocks of 80×80 pixels. Several color indices including red, green, and blue chromatic coordinates (*rgb*), contrast indices $r-g$, $g-b$, $(g-b)/|r-g|$ and $2g-r-b$, and hue, saturation, and intensity (*HSI*) were used as color descriptors. An artificial neural network was used in classification between the healthy and BLS-infected plants. The algorithm correctly recognized 79.23% of diseased leaves and 89.92% of healthy plants. Influence of the neural network architecture on the identification accuracy was also observed.
Key words: Cassava, brown leaf spot disease, image analysis, artificial neural network

INTRODUCTION

Brown leaf spot (BLS) disease caused by *Cercosporidium henningsii* Allesch is of fungal disease in cassava (*Manihot esculenta* Crantz) widely spread in Thailand. The symptoms appear as small brown spots with dark borders on the upper leaf surfaces (Msikita et al., 2000). The disease is usually considered less destructive comparing with other diseases such as cassava mosaic disease (CMD) or cassava bacterial blight (CBB). Nevertheless, infection of the BLS disease can cause leaf chlorosis and extensive defoliation which in turn resulting in yield loss up to 20% (Hillocks and Wydra, 2002; Teri et al., 1980). Furthermore, the infection of a plant may influence the susceptibility to another disease. Wydra and Verdier (2002) found a significant positive correlation between the incidence of cassava anthracnose disease (CAD) and the occurrence of BLS, as well as implications among the BLS, white leaf spot (WLS) and root rots. The authors additionally pointed out that the incidence of BLS is more prevalent in humid ecozones while its severity seemed to be increasing with number of surrounding trees and on profusely branching varieties. These clearly suggested that the BLS disease should not be neglected particularly in the conditions of Thailand.

Serveilance operation of the disease based on human inspection in large cassava fields may be difficult, especially when site-specific management is required. The use of an automated monitoring system which provides early detection with traceability of spatial and temporal propagation of the disease was considered an effective approach in long term.

A number of machine vision systems relying on different image processing techniques have been developed for different tasks in agriculture. Many of which focused on weeds detection (Woebbecke et al., 1995a; Woebbecke et al., 1995b; Yang et al., 2000;

Pérez et al., 2000; Yang et al., 2002; Gebhardt et al., 2006; Meyer and Camargo Neto, 2008). Bruno et al. (2008) obtained fractal dimension from digital images for plant taxonomy, similar to Backes and Bruno (2009), while Ketipearachchi and Tatsumi (2000) and Izumi and Iijima (2002) used it to characterize morphology of plants roots systems.

In the diagnosis of crop pests and diseases, the computer vision has been applied to identify fall armyworm damaged maize plants (Sena et al., 2003), Black Sigatoka infected banana leaves (Camargo and Smith, 2009a), and cotton crops damaged by Southern green stink bug, Bacterial angular, and Ascochyta blight (Camargo and Smith, 2009b). Wang et al. (2008) introduced a segmentation method for diseased leaf images. Application of machine vision on cassava diseases is, however, relatively few. To our knowledge, only Aduwo et al. (2010) proposed an image analysis technique to classify CMD-infected cassava leaves.

The objective of the present study was to develop an image analysis technique which is capable of recognizing visible symptoms of cassava BLS disease in actual field conditions.

MATERIALS and METHOD

Experimental site and plant materials

Image of cassava leaves were sampled from an experimental field located in Kamphaengsaen Campus of Kasetsart University, Nakhon Pathom, Thailand (Lat 14°2′11″N and Long 99°57′56″E). The variety of cassava plants was Rayong 5 which is of medium cultivar in terms of BLS disease tolerance. The age of the plants at sampling was 6 months at which time their canopy had fully developed. The BLS-infected plants were found scattering naturally throughout the field without systematic inoculation treatment.

Image aquisition, processing, and classification

Color images of cassava leaves were captured at several randomly chosen positions above the plants using a digital camera. The camera was set to operate in the automatic mode with a resolution of 640×480 pixels under natural sunlight at solar noon. The image set consisted of 80 images of healthy leaves, and 80 images that contain diseased leaves.

The Image Processing Toolbox™ for MATLAB® was used to pre-process and analyze the captured images. The original image were automatically cropped into 48 blocks of 80×80 pixels each. An image therefore presented 6 rows of blocks with 8 blocks on each row. The images which include diseased leaves when cropped into blocks, however, would result in both non-diseased (e.g. healthy, stems) and truely diseased regions (Figure 1). Counting of these blocks gave a total number of 5270 blocks for healthy, and 2410 blocks for diseased leaves. The primary red, green, and blue (RGB) color intensities of each single pixel were then obtained for futher transformation to other indices.

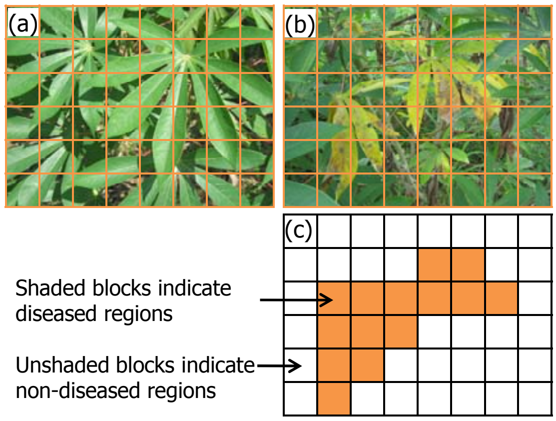

Figure 1. Sample images of: (a) healthy leaves, (b) diseased leaves, and (c) diseased regions mapping

Different color indices introduced by Woebbecke et al. (1995a) were used in this study. These included chromatic coordinates (r, g, and b) which are defined as:

$$r = \frac{R^*}{R^* + G^* + B^*},\ g = \frac{G^*}{R^* + G^* + B^*},\ b = \frac{B^*}{R^* + G^* + B^*}$$

where

$$R^* = \frac{R}{R_m},\ G^* = \frac{G}{G_m},\ B = \frac{B}{B_m}$$

and R_m, G_m, and B_m = 255, are the maximum tonal value for each primary color.

Contrast indices including $r - g$, $g - b$, $(g - b)/|r - g|$ and $2g - r - b$ were obtained to distinguish leaves and plant parts of different color. Preliminary test indicated the possibility of obtaining a zero in the denominator of the index $(g - b)/|r - g|$, denominator values between –0.01 and +0.01 were set to 0.01.

The hue, saturation, and intensity (HSI) color space was also used in addition to the chromatic coordinates. Modifed hue (H), saturation (S) and intensity (I) are derived from RGB values as follows:

$$H = \cos^{-1}\left[\frac{2R - G - B}{2\left[R^2 + G^2 + B^2 - RG - GB - RB\right]^{1/2}}\right] \quad (1)$$

for B ≤ G, otherwise $H = 360° - H$,

$$S = 1 - \frac{3}{(R + G + B)}[\min(R, G, B)] \quad (2)$$

and

$$I = \frac{1}{3}(R + G + B) \quad (3)$$

Mean value of each color index was calculated across the total 640 pixels (80×80) for each block and used as a representive value for further classification.

The artificial neural network (ANN) was used in classification between healthy and diseased leaves. The ANN model was a fully-connected feed-forward topology consisting of 10 inputs coresponding to ten color indices, and 2 output neurons representing healthy and diseased leaves (Figure 2). In order to search for the most optimal architecture, the classification accuracy was observed when the number of hidden neurons was varied from 10 to 100 for every increment of 10 neurons.

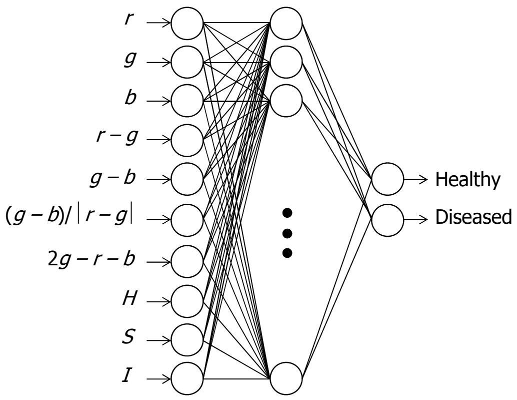

Figure 2. The ANN architecture for classification of healthy and diseased plants

A logistic sigmoid activation function was used in hidden neurons while a linear function was used in the output nodes. From the total 5270 samples of healthy plants, 3247 of which were randomly selected for training of the ANN while the rest were used for testing. Likewise, 1553 out of 2410 samples of diseased plants were used for training and the rest were spared for verification. All data was normalized into a range of 0.1–0.9. The target outputs were set to a value of 0.9 for the output node that corresponds to its category while the remaining was assigned to activate a value of 0.1. Training of the ANN was implemented by Levenberg-Marquardt algorithm to the mean squared error of 1.0×10^{-4} using Neural Network Toolbox™ for MATLAB®.

Brier score was used to evaluate the recognition ability of the ANN with different numbers of hidden neurons. Brier score is a unitless index and its range is from 0 to 1. The smaller the score is, the better is the recognition ability of the ANN.

RESULTS and DISCUSSION

The color indices of healthy and diseased leaves images have been obtained. Since the indices *rgb* and *HSI* theoritically range from 0 to 1, the ranges of these indices given in Table 1 thus demonstrated that the data used in this study was adequately entensive which confirmed the generality of the technique. The modified hue fell into a range of approximately 0.1 to 0.4. These respectively conrespond to the hue angle between 36 and 144° which are the sectors of yellow to green colors.

Table 1. Ranges of color indices

Indices	Ranges of index values	
	Healthy plants	Diseased plants
r	0.1044 – 0.7790	0.1325 – 0.9184
g	0.1419 – 0.9359	0.1808 – 0.9771
b	0.0617 – 0.7358	0.0261 – 0.6790
$r - g$	–0.3036 – 0.0539	–0.2793 – 0.0842
$g - b$	0.0282 – 0.4880	0.0409 – 0.5425
$(g - b)/\lvert r - g\rvert$	0.1579 – 10.5600	0.5315 – 26.7671
$2g - r - b$	0.0187 – 0.7548	0.0548 – 0.7469
H	0.1049 – 0.4382	0.1117 – 0.3993
S	0.0673 – 0.8432	0.1081 – 0.9439
I	0.1168 – 0.7882	0.1168 – 0.8370

Comparision between index values of healthy and diseased leaves is shown in Figure 3. The green coordinate was more or less the same. The red coorniate of diseased leaves was greater than that of healthy leaves while the coordinate blue resulted in the opposite. These are reasonable because the spots appear in brown color. The $r - g$ index for both healthy and diseased leaves had values that were often negative. When the indices were conbined as a ratio index $(g - b)/\lvert r - g\rvert$, better contrast between

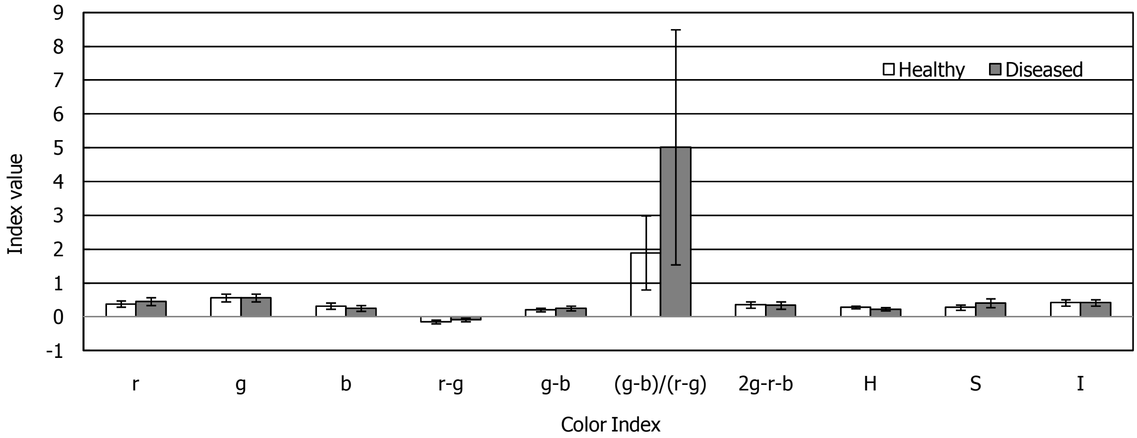

Figure 3. Comparison of index values of healthy and diseased leaves. Error bars represent standard deviation from the mean

the healthy and diseased leaves was obtained, but with increased standard deviation. Such result is very similar to the findings of Woebbecke et al. (1995a) though in their study the index was used to distinguish between plant and background. The present result thus suggested that the ratio index is still applicable to distinguish the healthy and diseased leaves even though in which case its contrast may be smaller than that between the plant and background. Modified hue of diseased leaves was lower than healthy leaves, indicating the approach of color towards yellow region. The modified hue and saturation showed some promise for separation of diseased leaves. The intensity was nearly the same and hence may not be a good parameter.

The ANN have been trained using different different numbers of hidden neurons. Actual activations of the neural network did not reach their extreme target values neither the lowest value of 0.1 nor the highest value of 0.9. However, the predictions were obviously classifiable if a threshold value of 0.5 was applied. The highest recognition accuracy of healthy leaves was 89.92% with 20 hidden neurons, while the highest possible accuracy for the diseased leaves was 79.23% with 30 hidden neurons (Table 2). It is notable that a high classification accuracy for a class may be attained but with a repay of obtaining lower accuracy for the other class. Several trials showed that the ANN could adequately learned the relationships with one hidden layer of only 10 neurons. Increasing the number of hidden neurons seems to have no effect on the classification accuracy. Using hidden neurons more than 20 nodes was therefore considered unnecessary. Evaluation of total classification performance based on Brier score confirmed that the ANN with 20 hidden neurons was the best architecture for the circumstances of this study.

Table 2. Number of hidden neurons and classification accuracy of healthy and diseased cassava leaves

Number of hidden neurons	Success classification (%)		Brier score
	Healthy plants	Diseased plants	
10	87.94	77.13	0.1528
20	89.92	75.73	0.1431
30	86.70	79.23	0.1552
40	88.68	77.48	0.1465
50	87.49	77.36	0.1552
60	88.04	78.06	0.1493
70	89.77	74.21	0.1486
80	87.35	78.18	0.1538
90	87.59	77.25	0.1549
100	87.05	77.36	0.1583

The present study showed a feasibility to detect the visible symptoms of BLS-infected cassava plants under field conditions by means of the machine vision. Considering from the porportion of training and test data set (62.5% for training and 37.5% for testing), the ANN was satisfactorily performed. The study results, nevertheless, suggested some possibility of misidentification of the diseased plants. This is likely to have been occurred due to many reasons. First, the study attempted to analyze the images without segmentation of leaves from background prior to detect the spots on the leaves. Maintaining of the background could therefore caused misleading color representation of actual healthy leaves and background which can be any from stems, soil, weeds, or residues. Second, the method did not taken into consideration the stage of disease infection or, in the other words, the degree of leaves damage. Obseravation indicated that the algorithm tended to detect yellowish leaves rather than really detecting the brown spots on leaves. Therfore, the classification would be correct only if the plants has already reached a high level damage. The early stages of infection at which the brown spots have appeared wherese the leaves are still green, can result in incorrect identification. Misclassification of the diseased plants may also be attributed to the illuminating condition in the cassava fields. Although the more robust color model such as HSI was used, however, variation of natural lighting was unavoidable. This can also depends on camera position relative to the cassava canopy and shading due to occlusion among the leaves. In order to improve the recognition ability, these issues must be taken in account associated with a more elaborate representation and interpretation of details in the images.

CONCLUSIONS

An image analysis technique relied on different color indices associated with neural network classification has been proposed for in situ detection of brown leaf spot disease in cassava. The results showed a feasibility of detecting visible symptoms of BLS-infected cassava plants in general. The algorithm correctly recognized 79.23% of diseased leaves and 89.92% of healthy plants. Futher improvement of the method should be done by incorporating the effects of infection stage, lighting condition, associated with a proper segmentation of leaves from backgrounds.

REFERENCES

Aduwo, J.R., E. Mwebaze, and J.A. Quinn, 2010. Automated Vision-Based Diagnosis of Cassava Mosaic Disease. Workshop on Data Mining in Agriculture (DMA 2010), Berlin.

Backes, A.R. and O.M. Bruno, 2009. Plant leaf identification using multi-scale fractal dimension. *In:* Foggia, P., C. Sansone, and M. Vento (Eds.), ICIAP 2009, LNCS 5716, pp. 143–150.

Bruno, O.M., R.O. Plotze, M. Falvo, and M. Castro, 2008. Fractal dimension applied to plant identification. Information Sciences, 178: 2722–2733.

Camargo, A. and J.S. Smith, 2009a. An image-processing based algorithm to automatically indentify plant disease visual symptoms. Biosystems Engineering, 102: 9–21.

Camargo, A. and J.S. Smith, 2009b. Image pattern classification for the identification of disease causing agents in plants. Computers and Electronics in Agriculture, 66: 121–125.

Gebhardt, S., J. Schellberg, R. Lock, and W. Kuhbauch, 2006. Identification of broad-leaved dock (Rumex obtusifolius L.) on grassland by means of digital image processing. Precision Agriculture, 7: 165–178.

Hillocks, R.J., and K. Wydra. 2002. Bacterial, fungal and nematode diseases. *In:* Hillocks, R.J., J.M. Thresh, and A.C. Bellotti (Eds.), Cassava: Biology, Production and Utilization. CAB International, UK.

Izumi, Y. and M. Iijima, 2002. Fractal and multifractal analysis of cassava root system grown by root-box method. Plant Production Science, 5(2): 146–151.

Ketipearachchi, K.W. and J. Tatsumi, 2000. Local fractal dimensions and multifractal analysis of the root system of legumes. Plant Production Science, 3(3): 289–295.

Meyer, G.E. and J. Camargo Neto, 2008. Verification of color vegetation indices for automated crop imaging applications. Computers and Electronics in Agriculture, 63: 282–293.

Msikita, W., B. James, E. Nnodu, J. Legg, K. Wydra, and F. Ogbe. 2000. Disease control in cassava farms. International Institute of Tropical Agriculture, Nigeria.

Pérez, A.J., F. López, J.V. Benlloch, and S. Christensen, 2000. Colour and shape analysis technique for weed detection in cereal fields. Computers and Electronic in Agriculture, 25: 197–212.

Sena Jr., D.G., F.A.C. Pinto, D.M. Queiroz, and P.A. Viana, 2003. Biosystems Engineering, 85: 449–454.

Teri, J.M., H.D. Thurston, J.C. Lozano, 1980. Effect of brown leaf spot and Cercospora leaf blight on cassava production. Tropical Agriculture, 57(3): 239–243.

Wang, L., T. Yang, and Y. Tian, 2008. Crop disease leaf image segmentation method based on color features. *In:* Daoliang, L. (Eds.), Computer and Computing Technologies in Agriculture, Vol.1. Springer, Boston. pp. 713–717.

Woebbecke, D.M., G.E. Meyer, K. Von Bargen, and D.A. Mortensen, 1995a. Color indices for weed identification under various soil, residue, and lighting conditions. Transactions of the ASAE, 38(1): 259–269.

Woebbecke, D.M., G.E. Meyer, K. Von Bargen, and D.A. Mortensen, 1995b. Shape features for identifying young weeds using image analysis. Transactions of the ASAE, 38(1): 271–281.

Wydra, K., and V. Verdier, 2002. Occurrence of cassava diseases in relation to environmental, agronomic and plant characteristics. Agriculture Ecosystems and Environment, 93: 211–226.

Yang, C.-C., S.O. Prasher, J.-A. Landry, and R. Kok, 2002. A vegetation localization algorithm for precision farming. Biosystems Engineering, 81: 137–146.

Yang, C.-C., S.O. Prasher, J.-A. Landry, H.S. Ramaswamy, and A. Ditommaso, 2000. Application of artificial neural networks in image recognition and classification of crop and weeds. Canadian Agricultural Engineering, 42: 147–152.